Influence of wind turbine mounted on vehicle on aerodynamic drag and energy gain

Ahmet Yildiz [1,] *, Besir Dandil [2]

[1] Faculty of Engineering, Department of Mechatronics Engineering, Firat University, 23119 Elazig, Turkey

[2] Faculty of Engineering, Department of Mechatronics Engineering, Iskenderun Technical University, 31200 Hatay, Turkey; besir.dandil@iste.edu.tr

***** Correspondence: ayildiz@firat.edu.tr

Abstract: This study aims to generate electrical energy using a wind turbine mounted in the front of a vehicle. In this study, the impact of the wind turbine on vehicle aerodynamics is evaluated, particularly in terms of aerodynamic drag, pressure, and flow velocity, while highlighting the potential benefits of energy production. The results showed that the aerodynamic drag coefficient of the vehicle increased by approximately 0.38% due to the wind turbine. However, the net energy gain produced by the wind turbine mounted on the vehicle while the vehicle is moving at a speed of 27 m/s was observed to be approximately 6.51% of the aerodynamic energy loss of the master model vehicle. In conclusion, this type of wind turbine system has the potential to enhance fuel efficiency and reduce environmental pollution. This study demonstrates that the use of wind turbines in electric vehicles can have positive effects on energy management.

Keywords: aerodynamic; aerodynamic drag coefficient; aerodynamic energy loss; computational fluid dynamics; vehicle; wind turbine

1. Introduction

Air pollution and the supply of clean energy are important for all countries and people in the world. Fossil fuels are generally used for the supply of energy in the world. Similarly, fossil fuels in the transportation sector occupy a significant amount of fuel consumption and are regarded as one of the major causes of air pollution [1]. The by-products produced during the combustion of fossil fuels cause global warming and pose a great threat to humans and especially children's health and future generations [2]. In addition, solutions with new and efficient energies are required in order to reduce the operating costs of vehicles coupled with increases in oil prices [3]. During the supply of energy, the world is polluted because of continuous and uncontrolled emissions due to the dangerous and polluting elements that are usually thrown into the atmosphere. One of the most important contributing factors is the combustion of fossil fuels in industrial and transportation sectors. The world is constantly

and uncontrollably polluted as a result of the burning of fossil fuels in the industrial and transportation sectors. Moreover, fossil fuels are limited, and their prices are increasing steadily as a result of increasing demand [4]. There are studies on various alternatives to reduce fossil fuel consumption and pollution emissions worldwide [5]. One of these studies is the realization of designs that have lower emissions and reduce environmental pollution in internal combustion vehicles where fossil fuels are used. In this context, taking into account the potential world energy crisis and its contribution to the solution of greenhouse gas formation, electric vehicles (EVs) have gained considerable attention in the last decade [6]. For this purpose, with the aim of using renewable energies in the transportation sector and eliminating exhaust emissions, it will contribute to the use of clean energy by turning to vehicles that use green energy [7]. Manufacturers have investigated the use of renewable energy sources to reduce the fossil fuel consumption of vehicles and to reduce the share of environmental pollution by utilizing renewable energy sources and to reduce air resistance losses. Thus, since there are no exhaust fumes in electric vehicles running with renewable energies, it will contribute to the air quality in the cities and hence to the health of people. In addition, the energy use efficiency of electric vehicles is higher than that of internal combustion engine-powered vehicles and this provides additional advantages for electric vehicles in terms of energy gain. In general, a large part of the fuel energy is consumed as friction and heat losses in internal combustion vehicles. Due to the fewness of power train in electric vehicles, the motor is smaller and it works more efficiently according to internal combustion engine [8].

For electric and hybrid vehicles, studies are generally carried out on energy management, power train and power distribution [9-13]. Some of these studies have investigated the optimum power distribution and the driving range of the vehicle and the life-cycle of the energy storage system depending on the batteries for electric and hybrid vehicles [14-16]. Electric vehicles are powered by electricity stored in batteries, fuel cells and ultra-capacitors [17-18]. Electricity supply is usually met by conventional electricity generation techniques. In recent years, renewable energy sources have gained importance and studies on the application of these resources to electric vehicles continue [19-21]. Regarding the energy gain, regenerative braking and thermoelectric generators have also gained importance in electric vehicles [22]. In the twentieth century, vehicle technology such as integrative technology and control technology is developing rapidly. Limiting driving distance is still an obstacle to the development of electric vehicles. This problem can be solved by regenerative braking. This method has become one of the ways to improve the driving range as it can

increase the driving range of an EV by 8-25% [23]. In the energy management system for hybrid vehicles, batteries can be charged at a certain rate during regenerative braking. In hybrid vehicles, energy can be stored in the batteries with the braking energy and can supply continuous energy depending on the charge and discharge time cycle [24]. Electric vehicles are largely dependent on energy storage technologies. For this reason, electric vehicles usually need to be connected to the grid with current technology. This will cause charging problems due to the need for additional energy for electric vehicles to make driving range long. The electrical energy supplied with the help of renewable energy sources can be used to operate the electrical motor stored in battery systems and other storage systems and to operate the basic systems for the operation of the vehicle [25].

The energy consumption of vehicles is generally examined in two categories: urban and extra-urban traffic. In urban traffic, since the vehicles generally act as stop-and-go, the temporary situation action of the vehicle is more dominant. In extra-urban traffic, since the vehicles usually move at constant and high speeds, the steady state action of the vehicle comes to the fore in this type of travel. The most important loss component of vehicles in extra-urban travel emerges as aerodynamic losses. The determination of the force and moment system affecting the moving vehicle, the properties of the flow around the vehicle, and thus the aerodynamic characteristics determination of the vehicle is one of the main problems of aerodynamics. A passenger car with a speed of 100 km/h spends 60% of its power to defeat the drag resistance force. By improving the aerodynamic properties of the vehicle, a significant reduction in fuel consumption is supplied [26]. Since aerodynamic losses increase quadratically with the speed of the vehicle, many studies have been made in the literature to improve the aerodynamic properties of vehicles [27-30].

In order to improve the performance of the vehicle and minimize the fuel consumption, the resistances acting on the vehicle must be reduced. Many studies have been done experimentally and numerically on improvement of vehicle aerodynamics [31-33]. In a study conducted by Kieffer et al. the front and side wings of a racing car were analyzed by Star-CD CFD (computational fluid dynamics) which uses the k-ε model, and examined the flow for different attack angles and ground effect [34]. Dong Sun et al. developed an electrically operated small aircraft as a result of aerodynamic experiments. They tested two types of winged body prototypes in wind and water tunnels. They concluded that the triangle model has a higher lift coefficient than the square, less vortex and thus better dynamic performance [35]. Xiang et al. conducted experimental studies in a wind tunnel to examine the aerodynamic properties of moving vehicles under cross winds. They determined the effect of

these factors on the aerodynamic properties of the vehicle by determining the forces acting on the vehicle at different wind directions and velocities [36]. Chowdhury et al. determined the impact of its devices in the hood of a commercial vehicle on aerodynamic resistance and fuel consumption. They used a wind tunnel to determine the aerodynamic drag coefficient of the vehicle. The aerodynamic drag on the vehicle has been measured at different vehicle velocities and for different combinations. The results indicated that they could reduce aerodynamic drag with changes in the vehicle body [37]. Ozawa et al. examined the solar car in terms of aerodynamics. They used the MAC (Marker and Cell) method based on CFD, taking into account the pressure distributions on the surface for the analysis of the upper vehicle body design [38].

In this study, in order to recover some of the aerodynamic energy losses that occur during the movement of the vehicles, an alternative system is proposed to recover some of the aerodynamic loss energy and to convert the gained energy into electrical energy by using wind speed. As is known, a relative wind speed acts on the vehicle moving at a certain speed, especially in front of the vehicle, and this lost energy must be met in order to maintain the speed of the vehicle. The main motivation of this study is the idea that some of this energy, which is lost due to the wind hitting the front of the vehicles, could be recovered. In parallel with this purpose, the aerodynamic drag coefficient and energy loss of a vehicle of certain dimensions have been examined numerically. Then, a wind turbine has been mounted in the front of the vehicle in order to use the wind energy generated by air hitting the front of the vehicle during movement. Since the wind turbine has been mounted in the front of the vehicle, the aerodynamic drag coefficient of the vehicle has been recalculated to determine how much additional loss the proposed wind turbine formed. Also, the amount of energy to be generated from the mounted wind turbine has been calculated, and the net energy gain to be obtained has been determined numerically. Using the simulation results obtained, it has been determined at the end of the numerical calculations that a wind turbine to be mounted in the vehicle can recover 6.51% of aerodynamic losses. This recovered energy can be used to meet the electrical energy needs of the electric / hybrid vehicle or to charge the batteries of the vehicles. Thus, the vehicle can be driven for longer distances with the same battery group.

2. Materials and Methods

Aerodynamic drag is an important element in vehicle design. It has a direct effect on vehicle stability, driving comfort, and fuel consumption. In a vehicle with an average speed

of 100 km/h, about 75% of the resistances to movement are aerodynamic resistances. Therefore, the reduction of the aerodynamic drag coefficient is important for fuel consumption. Aerodynamic forces occur on objects with external airflow around them. The aerodynamic characteristics for these objects are expressed as the aerodynamic drag coefficient (C_d) and the aerodynamic lift coefficient (C_l). Because of the external geometric form of an object, the drag force (F_d) applied by the air flow in the direction of flow on the object acts on the vehicle surface in the direction of air flow. The drag force results in a dimensionless aerodynamic drag coefficient value, and the C_d constant depends on the shape of the object exposed to the air flow. Accordingly, the aerodynamic drag coefficient value with the help of drag force can be determined as [39]:

$$C_d = \frac{F_d}{\frac{1}{2}\rho V^2 A} \tag{1}$$

where F_d is the total drag force acting on the model, ρ is density of fluid, V is the free airflow speed, and A is the frontal area of body.

In the same way, the lifting force (F_l) applied in the direction perpendicular to the flow results in the dimensionless lift coefficient (C_l). The lift coefficient can be calculated as follows:

$$C_l = \frac{F_l}{\frac{1}{2}\rho V^2 A} \tag{2}$$

where F_l is the total lift force acting on the model.

The value of the aerodynamic characteristics varies depending on the surface geometric form of an object. As the dimensionless aerodynamic drag coefficient decreases, a significant decrease in energy consumption will be observed since the amount of energy that the objects will spend to overcome the air resistance will decrease. In most geometries, the drag coefficient remains constant at high Reynolds numbers. However, especially in Reynolds numbers less than 10^4, the aerodynamic drag coefficient depends on the Reynolds number. In the external flow, the Reynolds number can be expressed as follows:

$$\mathrm{Re} = \frac{\rho V L}{\mu} \tag{3}$$

The energy consumed (E_d) against the aerodynamic drag force at the travelled distance (s) during the movement of the vehicle can be expressed as [40]:

$$E_d = F_d s = \frac{1}{2} C_d \rho A V^2 s \tag{4}$$

The amount of power generated in the wind turbine system can be calculated as,

$$P = \frac{1}{2} C_p \rho A V^3 \tag{5}$$

where C_p is power coefficient.

The flow is generally considered to be three-dimensional, isothermal, incompressible, viscous, and turbulent when the external flow in vehicles is examined. Thus, the Navier - Stokes equations, which include continuity and momentum equations, are used to define the external flow area [41]. In practice, it is difficult to solve these equations analytically. Therefore, these equations are solved numerically using package programs.

3. Numerical Analysis

In this paper, it is aimed to perform a numerical study of aerodynamic effects and energy loss in a particular vehicle and to recover some of the energy loss with the help of a wind turbine mounted on the vehicle. For this purpose, a specific vehicle was designed and modeled with SolidWorks.

Numerical analysis of the front part of the vehicle designed according to the grid and wind turbine status was carried out using ANSYS Fluent. Then, the aerodynamic drag coefficient, velocity, and pressure distributions of each vehicle model were examined. The amount of energy loss of each vehicle model and the amount of energy produced with the help of the wind turbine were calculated. The flow chart of numerical analysis is shown in Figure 1.

3.1. Modeling of the Vehicle

In this paper, vehicle models to be modeled for flow analysis were designed by surface modeling with the help of SolidWorks, mesh process and analyses were done using ANSYS Fluent. The vehicle model shown in Figure 2 is designed to study the aerodynamic effects in the proposed vehicle model with wind turbine.

The necessary modifications have been made to the designed vehicle model for the analysis of the formation of aerodynamic effects on the propeller to be mounted on the vehicle. In the designs, the master model vehicle is defined as MMV, and the vehicle model with wind turbine is defined as VMWT. When designing the MMV, as shown in Figure 3, grids were placed on the central surface on the front surface of the model, on a total area of

60x30 cm. To discharge the air inside the hood of the vehicle, three air discharge ducts of 14x25 cm size have been formed on both sides of the vehicle, as shown in Figure 3.

Then, a 50 cm diameter hole was drilled on the front surface of the vehicle as shown in Figure 4, and it is aimed to recover some of the aerodynamic losses with the help of wind energy with the system created in this way.

3.2. Grid Generation for CFD Simulation

Vehicle models modeled the SolidWorks are imported to the geometry module of Fluent software in ANSYS to create solution geometry. Vehicle views created for the purpose of solution geometries in Fluent software are given in Figure 5.

In order to simulate a passenger vehicle moving on a real road, the flow area is designed as shown in Figure 6.

The wind tunnel area was created as shown in Figure 7 to analyze the flow around the vehicle. The air inlet surface is designated as inlet, the air outlet surface is designated as outlet and the remaining surfaces are designated as wall. The size of the computational domain has been chosen so that the aerodynamic force is not affected by the area size. In order for the analysis to give accurate results, the air volume is taken as a minimum distance of 3 vehicles in front of the vehicle and a distance of at least 5 vehicles behind it [39].

In this wind tunnel, a mesh structure has been formed with a dense mesh around the vehicle. The meshes have been generated using a multiblock diagram with triangular elements. A smaller size mesh has been used near the surfaces of the vehicle body in order to correctly analyze the flow in the boundary layer. In addition, a grid independence study has been carried out to determine that element size does not affect the results. The variation of the drag coefficient was investigated according to six different mesh structures. Grid independence studies have shown that the drag coefficient converges at approximately 689642 nodes and 3859758 elements. The relative error of the drag coefficient of the selected mesh according to the thinnest mesh is less than 0.5%. The generated mesh structures are shown in Figures 8 and 9.

3.3. Methodology for CFD Analysis

In this paper, the solution analysis of the models was done using ANSYS Fluent. In the study, the solution has been considered as three-dimensional, and the double precision has been activated in order to increase the accuracy of the analysis. In the method used for the solution, Reynolds-Averaged Navier-Stokes equations, including the continuity equation and momentum equation, are solved. For the SAE (Society of Automotive Engineers) standard

atmosphere, the analyses have been carried out in a steady state with a reference pressure of 101325 Pa and a temperature of the air of 15 °C, in adiabatic and completely turbulent conditions. These standard atmospheric conditions have been used in the calculation of density and viscosity.

The vehicle speed for the external flow has been taken as 27 m/s, and atmospheric pressure has been accepted for the outlet boundary condition. Accordingly, the reference velocity of the air flow has been determined as 27 m/s and Re = 7.39×10^6.

Since the rotation, boundary layers under the reverse pressure radians, separation, and recirculation containing flows provide superior performance, a k-ε model can be implemented around the walls. The k-ε turbulence model integrated into Fluent software has been proven to provide the best fit with experimental results [42]. The aerodynamic simulation condition of the vehicle has been accepted as turbulent. The solution properties are given in Table 1.

4. Results and Discussions

In this paper, static pressure contours, velocity contours, and aerodynamic drag coefficients of the MMV and VMWT have been determined using ANSYS-Fluent, and the obtained values are given in this section. The aerodynamic drag coefficient and aerodynamic drag force for the vehicle models as a result of the solution are given in Table 2.

Figure 10 shows a front view of the static pressure contours of the MMV and VMWT. As shown in the figure, the high pressure range is marked as red. The highest pressure value has occurred in the front of the vehicle as a result of the effect of air flow on the body of the vehicle. It has been observed that there is a lower air pressure in the windshield area of the vehicles. At the top of the vehicle models, there is a low-pressure zone marked in blue, leading to high air velocities. In addition, low pressure has occurred in the bottom of vehicle models and on the side surfaces.

In the analysis of the pressure distribution of the air around the vehicle body, it has been observed that the pressure losses in the front part of the vehicle constitute the main region. The results of the air pressure contour on the vehicle body revealed similar results to other existing studies [39].

The velocity views vectors of the MMV and VMWT are given in Figures 11 and 12, respectively. In addition, velocity streamlines for vehicle models are shown in Figures 13 and 14. It has been observed that there is a lower air velocity zone in the vehicle rear compared to the front of the vehicle. Also, the low speed zone was seen in the windshield area of the vehicle, and the reflected air streams circulate from the top surface to the rear air

gap. Meanwhile, the high speed zone has been seen at the exit of the roof area. This case can be caused by overlapping air streams in the top region of the vehicle [43].

Pressure and velocity contours from the cross section taken along the z axis of the vehicle models are given in Figure 15 and Figure 16, respectively.

For all vehicle models, it was observed that the flow in the air streams around the vehicle body was not distorted and there was no turbulent flow. Accordingly, the air flow separated from the front bumper region of the vehicle is continuously flowing as a laminar flow around the vehicle. Behind the rear of the vehicle, a virtual tail was formed due to the Kammback effect caused by air streams. According to the assumptions of the Kammback effect theory, the air stream creates the virtual tail of the vehicle. The air flowing towards the roof of the vehicle tended to connect with the air flowing towards the bottom of the vehicle. In these cases, velocity vectors in front of the vehicle exhibited local turbulence and turbulent flow. In addition, an asymmetric irregular air circulation has occurred around the modifications formed in the front of the vehicle.

The effect of aerodynamic drag coefficient on energy consumption and fuel consumption is important for vehicles. In this context, the effects of design modifications on aerodynamic energy gain and aerodynamic energy loss are presented. The technical specifications of the MMV are shown in Table 3.

4.1. Effect of Aerodynamic Drag Coefficient on Energy Consumption

The work done against the aerodynamic drag force can be expressed as in Eq. (4). Accordingly, the energy consumption of the models against aerodynamic force has been calculated with the help of Eq. (4) and is given in Figure 17. As seen in Figure 17, at a speed of 27 m/s, the aerodynamic energy consumption for the MMV is 75243 kJ, while it is 75533 kJ for the VMWT. This indicates an approximate increase of 0.38% in aerodynamic energy loss.

The power generated from the wind turbine in VMWT has been calculated using Eq. (5). The energy generated by the turbine has been determined by taking into account the driving time of the vehicle. In this case, the additional aerodynamic energy loss difference (E_{loss}) in the VMWT relative to the MMV, the energy generated (E_{tur}) by the wind turbine, and the energy gain (E_{gain}) of the WMWT compared to the MMV are shown in Figure 18. In this context, E_{loss} was calculated as 290 kJ, E_{tur} as 5192 kJ, and E_{gain} as 4902 kJ. Accordingly, it has been observed that the additional energy loss due to aerodynamic drag can be offset, and electrical energy can be generated using the wind turbine mounted on the vehicle. This

enables the recovery of aerodynamic energy loss by converting wind speed into electrical energy during vehicle movement. Consequently, this approach contributes to reduced fuel consumption, promoting more environmentally friendly vehicles in the transportation sector.

Additionally, the percentage of aerodynamic energy loss in the VMWT compared to the MMV is approximately 0.38%, while the percentage of energy gain from the turbine in the VMWT relative to the MMV is about 6.51%, as shown in Figure 19.

5. Conclusions

The main objective of this study is to generate electrical energy using a wind turbine mounted on the front part of a vehicle. Additionally, the effects of the wind turbine mounted on the vehicle on aerodynamic drag, pressure, and flow velocity have been investigated. The main findings are summarized below:

- Pressure and Flow Velocity Distributions: It was observed that the pressure was higher on the front surfaces where the vehicle was directly in contact with the wind during the movement. It was observed that velocity streamlines were formed covering the shapes of both vehicle models.
- Aerodynamic Drag Coefficient: The aerodynamic drag coefficient of the VMWT increased more compared to the MMV by 0.38% due to the air mass in the turbine region. The vortices caused by the wind turbine have a significant impact on the aerodynamics of the vehicle. By designing a suitable wind turbine, it is suggested that this increase in aerodynamic drag coefficient could be reduced below that of the simulation model.
- Energy Gain and Losses: At a vehicle speed of 27 m/s, the aerodynamic energy loss in VMWT increased by approximately 0.38% compared to MMV. However, the net energy gain generated by the wind turbine was about 6.51% of the aerodynamic energy loss of the MMV. This case shows that the wind turbine system can compensate for the additional aerodynamic energy loss and provide an energy gain.
- Hybrid Application and Future Prospects: This design can meet part of the energy consumption of the vehicle while in motion, regardless of environmental conditions. In electric vehicles, implementing this system may enable smaller battery sizes and contribute to reduced fuel consumption and environmental pollution.

Consequently, this study showed that the use of wind turbines in electric vehicles can have positive effects on energy efficiency.

Acknowledgements: Not applicable.

Author's Contributions: AY: Conceptualization, methodology, software, validation, formal analysis, writing - original draft, visualization; BD: Conceptualization, writing - review & editing, supervision.

Biographies:

Ahmet Yildiz received his BSc degree in Electrical and Electronics Engineering and Mechatronics Engineering (double major) from Firat University, Elazig, Turkey, in 2015. He received his MSc and Ph.D. degrees in Mechatronics Engineering from Firat University, in 2018 and 2023, respectively. He is currently a Research Assistant in the Department of Mechatronics Engineering at Firat University, Elazig, Turkey. His research interests include electric machine design and applications, renewable energy and mechatronics.

Besir Dandil is currently a Professor in the Department of Mechatronics Engineering at Iskenderun Technical University, Hatay, Turkey. He received his BSc, MSc and PhD degrees in Electrical and Electronics Engineering from Firat University, Elazig, Turkey, in 1992, 1998 and 2004, respectively. His current research interests include analogue and digital electronics, the power electronics, power quality, and control systems.

Funding: No applicable.

Competing Interests: The authors declare no conflict of interest.

References

1. Montazeri-Gh, M. and Mahmoodi-k, M. "Development a new power management strategy for power split hybrid electric vehicles", *Transportation Research Part D: Transport and Environment*, **37**, pp. 79–96 (2015). DOI: 10.1016/j.trd.2015.04.024.
2. Perera, F. "Pollution from Fossil-Fuel Combustion is the Leading Environmental Threat to Global Pediatric Health and Equity: Solutions Exist", *International Journal of Environmental Research and Public Health*, **15**(1), p. 16 (2018). DOI: 10.3390/ijerph15010016.
3. Shancita, I., Masjuki, H. H., Kalam, M. A., et al. "A review on idling reduction strategies to improve fuel economy and reduce exhaust emissions of transport vehicles", *Energy Conversion and Management*, **88**, pp. 794–807 (2014). DOI: 10.1016/j.enconman.2014.09.036.
4. Yıldız, A. and Dandıl, B. "Power Generation Potential of Small Wind Turbine in Elazig Province, Turkey", *2019 4th International Conference on Power Electronics and Their Applications (ICPEA)*, pp. 1–6 (2019). DOI: 10.1109/ICPEA1.2019.8911158.
5. Li, W., Yu, X., Hu, N., et al. "Study on the relationship between fossil energy consumption and carbon emission in Sichuan Province", *Energy Reports*, **8**, pp. 53–62 (2022). DOI: 10.1016/j.egyr.2022.01.112.
6. Muratori, M., Alexander, M., Arent, D., et al. "The rise of electric vehicles—2020 status and future expectations", *Progress in Energy*, **3**(2), p. 022002 (2021). DOI: 10.1088/2516-1083/abe0ad.
7. Bogdanov, D., Gulagi, A., Fasihi, M., et al. "Full energy sector transition towards 100% renewable energy supply: Integrating power, heat, transport and industry sectors including desalination", *Applied Energy*, **283**, p. 116273 (2021). DOI: 10.1016/j.apenergy.2020.116273.
8. Taghavipour, A., Vajedi, M., Azad, N. L., et al. "Predictive Power Management Strategy for a PHEV Based on Different Levels of Trip Information", *IFAC Proceedings Volumes*, **45**(30), pp. 326–333 (2012). DOI: 10.3182/20121023-3-FR-4025.00026.
9. Xiang, C., Huang, K., and Langari, R. "Power-Split Electromechanical Transmission Design and Validation with Three Planetary Gears for Heavy-Duty Vehicle", *Iranian Journal of Science and Technology, Transactions of Mechanical Engineering*, **42**(4), pp. 383–400 (2018). DOI: 10.1007/s40997-017-0105-1.
10. Ganesh, A. H. and Xu, B. "A review of reinforcement learning based energy management systems for electrified powertrains: Progress, challenge, and potential solution", *Renewable and Sustainable Energy Reviews*, **154**, p. 111833 (2022). DOI: 10.1016/j.rser.2021.111833.

11. Saiteja, P. and Ashok, B. “Critical review on structural architecture, energy control strategies and development process towards optimal energy management in hybrid vehicles”, *Renewable and Sustainable Energy Reviews*, **157**, p. 112038 (2022). DOI: 10.1016/j.rser.2021.112038.
12. Sidharthan, P. V., Kashyap, Y., and Vijay, C. R. “A review on hybrid source energy management strategies for electric vehicle”, *International Journal of Energy Research*, **45**(14), pp. 19819–19850 (2021). DOI: 10.1002/er.7107.
13. Wilberforce, T., Anser, A., Swamy, J. A., et al. “An investigation into hybrid energy storage system control and power distribution for hybrid electric vehicles”, *Energy*, **279**, p. 127804 (2023). DOI: 10.1016/j.energy.2023.127804.
14. Yang, Y., Xu, Y., Zhang, H., et al. “Research on the energy management strategy of extended range electric vehicles based on a hybrid energy storage system”, *Energy Reports*, **8**, pp. 6602–6623 (2022). DOI: 10.1016/j.egyr.2022.05.013.
15. Eckert, J. J., Barbosa, T. P., da Silva, S. F., et al. “Electric hydraulic hybrid vehicle powertrain design and optimization-based power distribution control to extend driving range and battery life cycle”, *Energy Conversion and Management*, **252**, p. 115094 (2022). DOI: 10.1016/j.enconman.2021.115094.
16. Bai, Y., Li, J., He, H., et al. “Optimal Design of a Hybrid Energy Storage System in a Plug-In Hybrid Electric Vehicle for Battery Lifetime Improvement”, *IEEE Access*, **8**, pp. 142148–142158 (2020). DOI: 10.1109/ACCESS.2020.3013596.
17. Farjam, T., Saadat Foumani, M., and Delkhosh, M. “Optimization of multiple transmission layouts for minimal energy consumption of a battery electric vehicle”, *Scientia Iranica*, **26**(4), pp. 2382–2393 (2019). DOI: 10.24200/sci.2018.20783.
18. Sagaria, S., Costa Neto, R., and Baptista, P. “Assessing the performance of vehicles powered by battery, fuel cell and ultra-capacitor: Application to light-duty vehicles and buses”, *Energy Conversion and Management*, **229**, p. 113767 (2021). DOI: 10.1016/j.enconman.2020.113767.
19. Nguefack, M. C. F., Fotso, B. E. M., and Fogue, M. “3D numerical investigation of the air flow in the wake of a compact SUV-type vehicle fitted with optimized horizontal Savonius turbines”, *Journal of the Brazilian Society of Mechanical Sciences and Engineering*, **45**(1), p. 17 (2022). DOI: 10.1007/s40430-022-03933-w.
20. Chowdhury, N., Hossain, C. A., Longo, M., et al. “Optimization of Solar Energy System for the Electric Vehicle at University Campus in Dhaka, Bangladesh”, *Energies*, **11**(9), p. 2433 (2018). DOI: 10.3390/en11092433.
21. Fathabadi, H. “Utilizing solar and wind energy in plug-in hybrid electric vehicles”, *Energy Conversion and Management*, **156**, pp. 317–328 (2018). DOI: 10.1016/j.enconman.2017.11.015.
22. Qiu, C. and Wang, G. “New evaluation methodology of regenerative braking contribution to energy efficiency improvement of electric vehicles”, *Energy Conversion and Management*, **119**, pp. 389–398 (2016). DOI: 10.1016/j.enconman.2016.04.044.
23. Cao, B., Bai, Z., and Zhang, W. “Research on control for regenerative braking of electric vehicle”, *IEEE International Conference on Vehicular Electronics and Safety*, pp. 92–97 (2005). DOI: 10.1109/ICVES.2005.1563620.
24. Thounthong, P., Chunkag, V., Sethakul, P., et al. “Comparative Study of Fuel-Cell Vehicle Hybridization with Battery or Supercapacitor Storage Device”, *IEEE Transactions on Vehicular Technology*, **58**(8), pp. 3892–3904 (2009). DOI: 10.1109/TVT.2009.2028571.
25. McDonough, M. “Integration of Inductively Coupled Power Transfer and Hybrid Energy Storage System: A Multiport Power Electronics Interface for Battery-Powered Electric Vehicles”, *IEEE Transactions on Power Electronics*, **30**(11), pp. 6423–6433 (2015). DOI: 10.1109/TPEL.2015.2422300.
26. Mohr, S. H., Wang, J., Ellem, G., et al. “Projection of world fossil fuels by country”, *Fuel*, **141**, pp. 120–135 (2015). DOI: 10.1016/j.fuel.2014.10.030.
27. Mohrfeld-Halterman, J. A. and Uddin, M. “High fidelity quasi steady-state aerodynamic model effects on race vehicle performance predictions using multi-body simulation”, *Vehicle System Dynamics*, **54**(7), pp. 963–981 (2016). DOI: 10.1080/00423114.2016.1175648.
28. Lee, S. W. “Computational analysis of air jet wheel deflector for aerodynamic drag reduction of road vehicle”, *Microsystem Technologies*, **24**(11), pp. 4453–4463 (2018). DOI: 10.1007/s00542-018-3992-1.

29. Ha, S. J., Chun, U., Park, J. Y., et al. “Enhancement of aerodynamic performance through high pressure relief in the engine room for passenger car using cfd technique”, *International Journal of Automotive Technology*, **18**(5), pp. 779–784 (2017). DOI: 10.1007/s12239-017-0077-6.
30. Cho, J., Kim, T.-K., Kim, K.-H., et al. “Comparative investigation on the aerodynamic effects of combined use of underbody drag reduction devices applied to real sedan”, *International Journal of Automotive Technology*, **18**(6), pp. 959–971 (2017). DOI: 10.1007/s12239-017-0094-5.
31. Laimon, A. L., Namasivayam, S. N., and Hosseini Fouladi, M. “The Development of an Optimal Aerodynamic Design for a Human Powered Vehicle”, *Iranian Journal of Science and Technology, Transactions of Mechanical Engineering*, **43**(1), pp. 797–807 (2019). DOI: 10.1007/s40997-018-0196-3.
32. Sadettin Hamut, H., El-Emam, R. S., Aydin, M., et al. “Effects of rear spoilers on ground vehicle aerodynamic drag”, *International Journal of Numerical Methods for Heat & Fluid Flow*, **24**(3), pp. 627–642 (2014). DOI: 10.1108/HFF-03-2012-0068.
33. Rehmat, A., Fayyaz, Bashmal, S., et al. “Numerical Modeling of the Shape Optimization for a Commercial Car by Decreasing Drag and Increasing Stability”, *Arabian Journal for Science and Engineering*, **48**(9), pp. 12427–12437 (2023). DOI: 10.1007/s13369-023-07834-5.
34. Kieffer, W., Moujaes, S., and Armbya, N. “CFD study of section characteristics of Formula Mazda race car wings”, *Mathematical and Computer Modelling*, **43**(11), pp. 1275–1287 (2006). DOI: 10.1016/j.mcm.2005.03.011.
35. Sun, D., Wu, H., Lam, C. M., et al. “Development of a small air vehicle based on aerodynamic model analysis in the tunnel tests”, *Mechatronics*, **16**(1), pp. 41–49 (2006). DOI: 10.1016/j.mechatronics.2005.09.004.
36. Xiang, H., Li, Y., Chen, S., et al. “A wind tunnel test method on aerodynamic characteristics of moving vehicles under crosswinds”, *Journal of Wind Engineering and Industrial Aerodynamics*, **163**, pp. 15–23 (2017). DOI: 10.1016/j.jweia.2017.01.013.
37. Chowdhury, H., Moria, H., Ali, A., et al. “A Study on Aerodynamic Drag of a Semi-trailer Truck”, *Procedia Engineering*, **56**, pp. 201–205 (2013). DOI: 10.1016/j.proeng.2013.03.108.
38. Ozawa, H., Nishikawa, S., and Higashida, D. “Development of aerodynamics for a solar race car”, *JSAE Review*, **19**(4), pp. 343–349 (1998). DOI: 10.1016/S0389-4304(98)00019-8.
39. El, E., Yildiz, C., Dandil, B., et al. “Effect of wind turbine designed for electric vehicles on aerodynamics and energy performance of the vehicle”, *Thermal Science*, **26**(4 Part A), pp. 2907–2917 (2022). DOI: 10.2298/TSCI2204907E.
40. Yildiz, A. and Dandil, B. “Investigation of effect of vehicle grilles on aerodynamic energy loss and drag coefficient”, Journal *of Energy Systems*, **2**(4), pp. 190–203 (2018). doi: 10.30521/jes.461133.
41. Muyl, F., Dumas, L., and Herbert, V. “Hybrid method for aerodynamic shape optimization in automotive industry”, *Computers & Fluids*, **33**(5), pp. 849–858 (2004). DOI: 10.1016/j.compfluid.2003.06.007.
42. Singh, S. N., Rai, L., Puri, P., et al. “Effect of moving surface on the aerodynamic drag of road vehicles”, *Proceedings of the Institution of Mechanical Engineers, Part D: Journal of Automobile Engineering*, **219**(2), pp. 127–134 (2005). DOI: 10.1243/095440705X5886.
43. Gopal, P. and Senthilkumar, T. “Influence of Wake Characteristics of a Representative Car Model by Delaying Boundary Layer Separation”, *Journal of Applied Science and Engineering*, **16**(4), pp. 363–374 (2013). DOI: 10.6180/jase.2013.16.4.04.

Figures and Tables

Figure 1. Flow chart of numerical analysis.

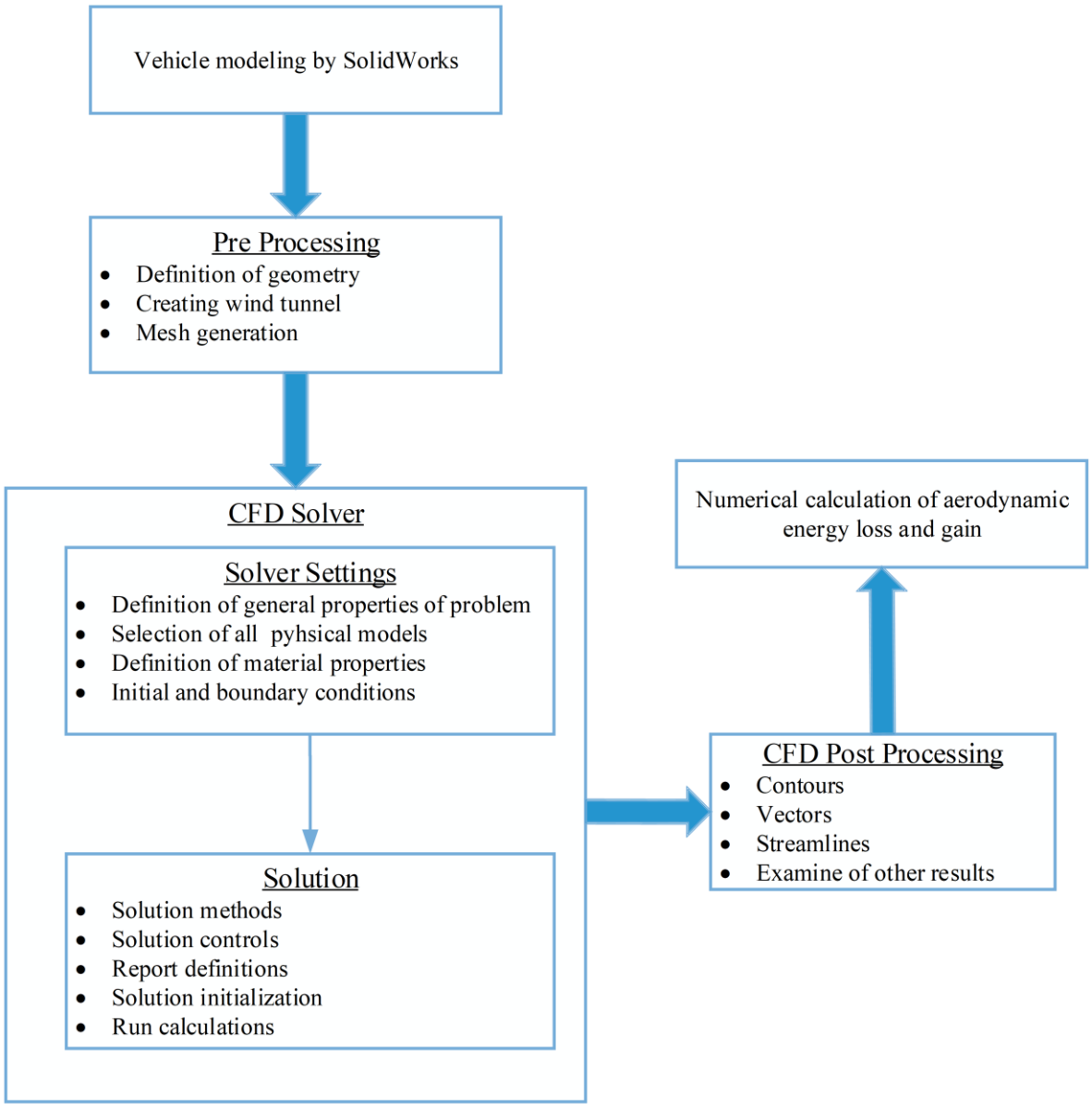

Figure 2. General views of the designed model vehicle.

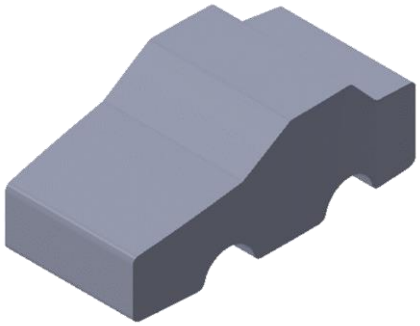

Figure 3. Front and side views of the MMV.

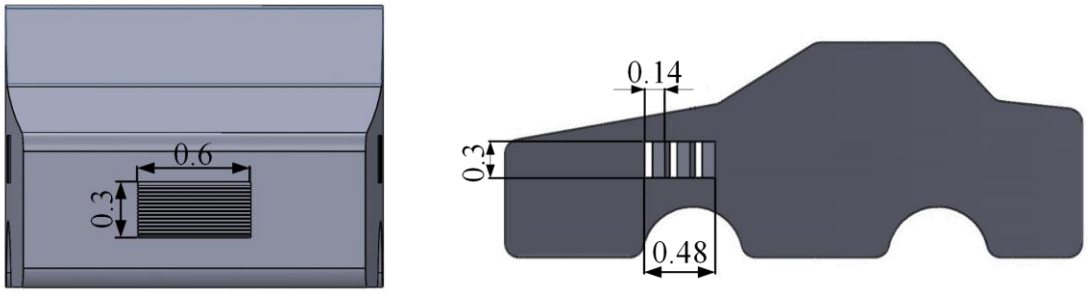

Figure 4. Modifications of the front part of the VMWT.

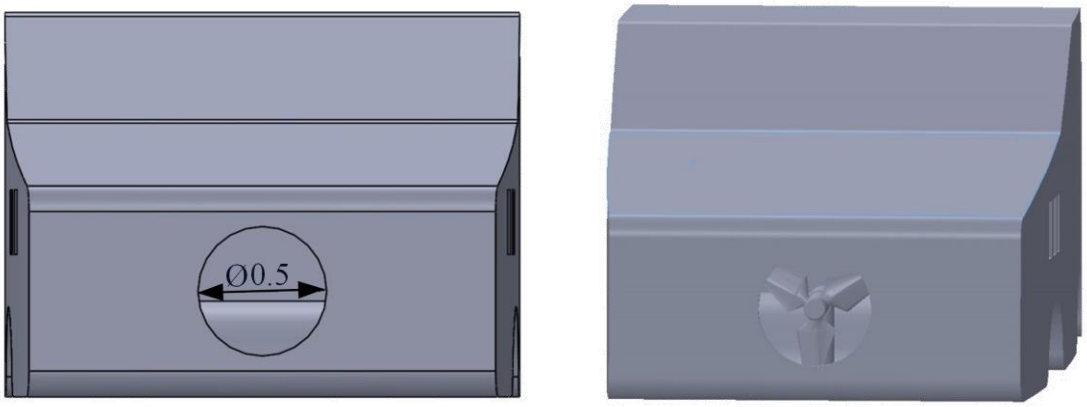

Figure 5. Isometric views of the MMV and the VMWT.

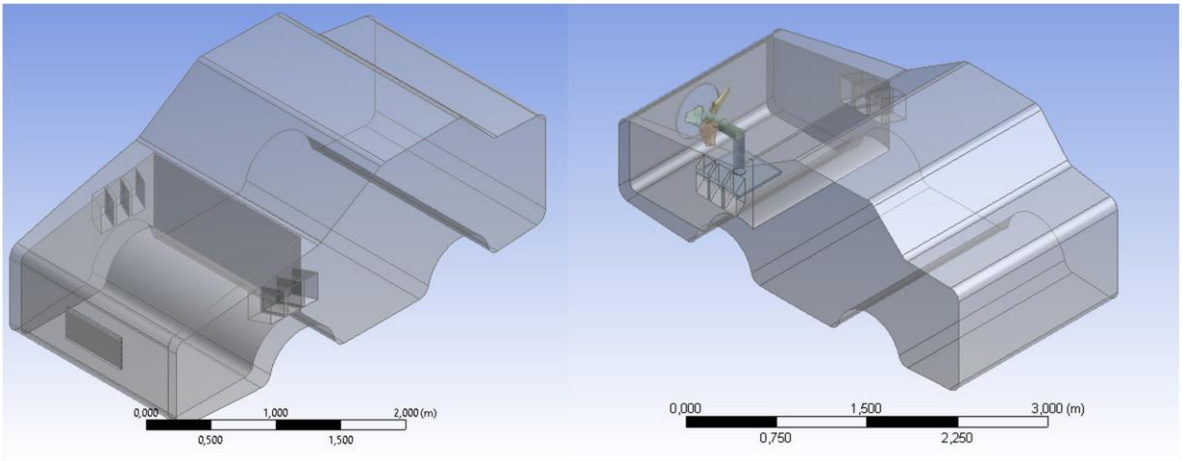

Figure 6. View of wind tunnel and designed model vehicle.

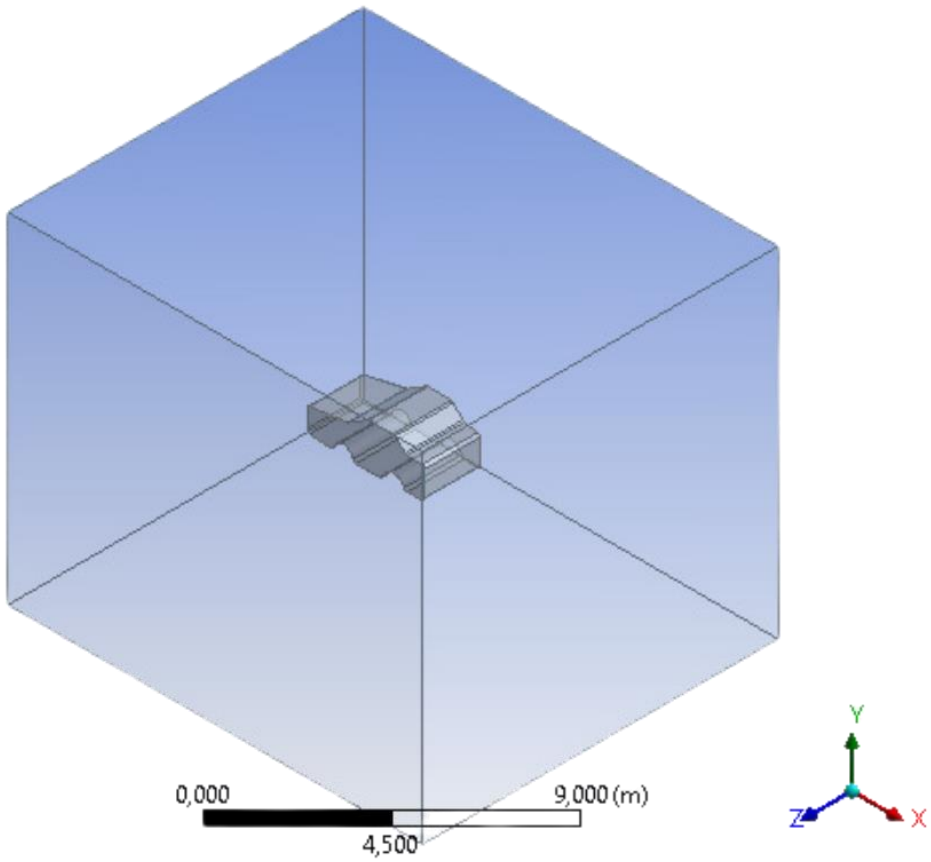

Figure 7. Inlet and outlet surfaces of the wind tunnel.

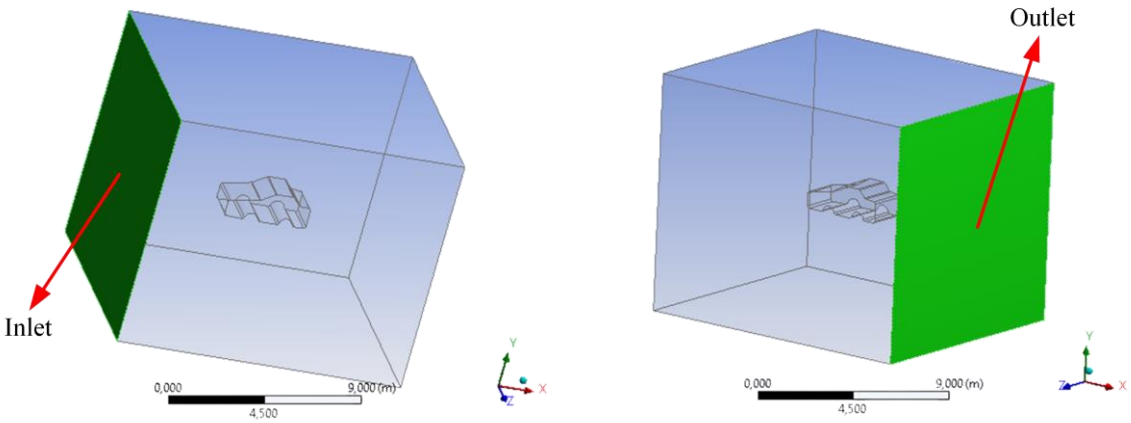

Figure 8. General mesh view of wind tunnel and vehicle.

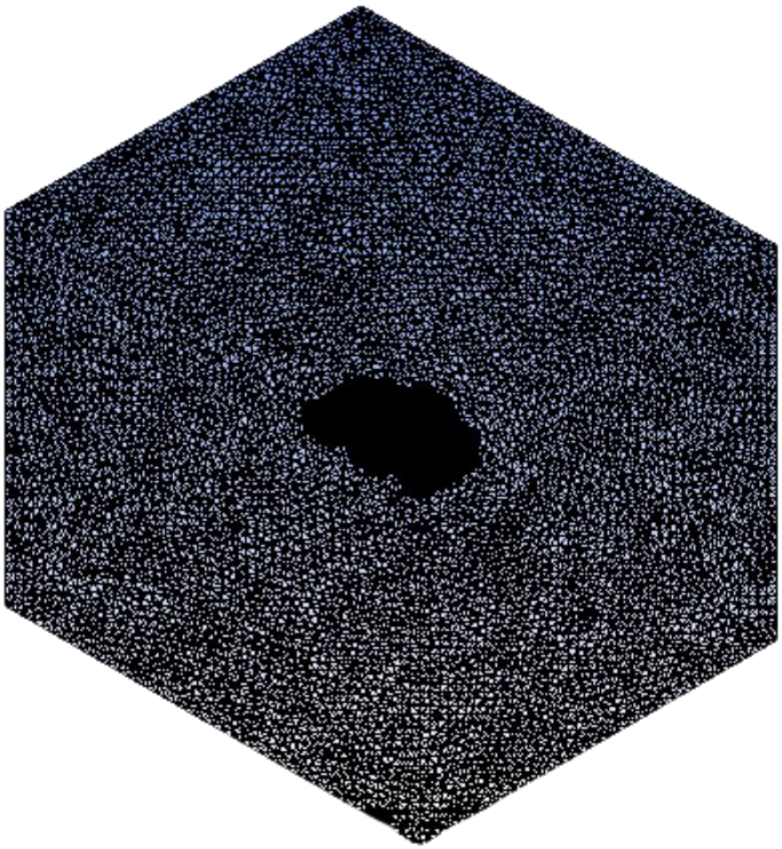

Figure 9. Mesh structures of MMV and VMWT.

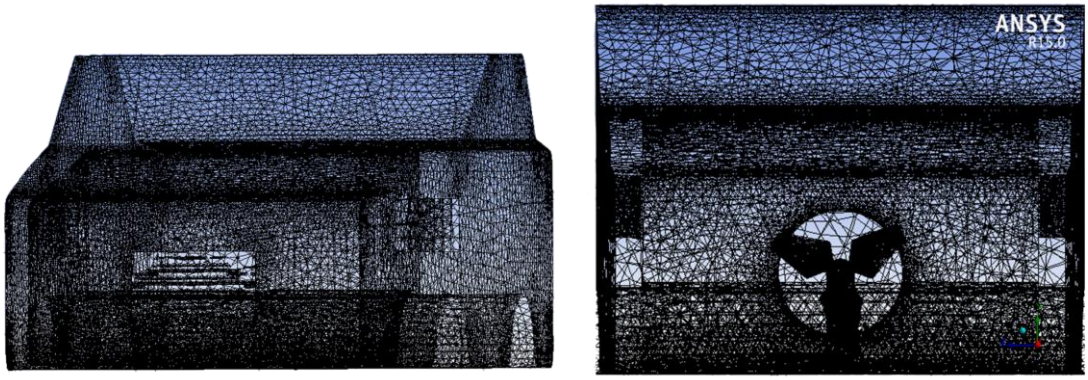

Figure 10. Static pressure contours (a) MMV, (b) VMWT

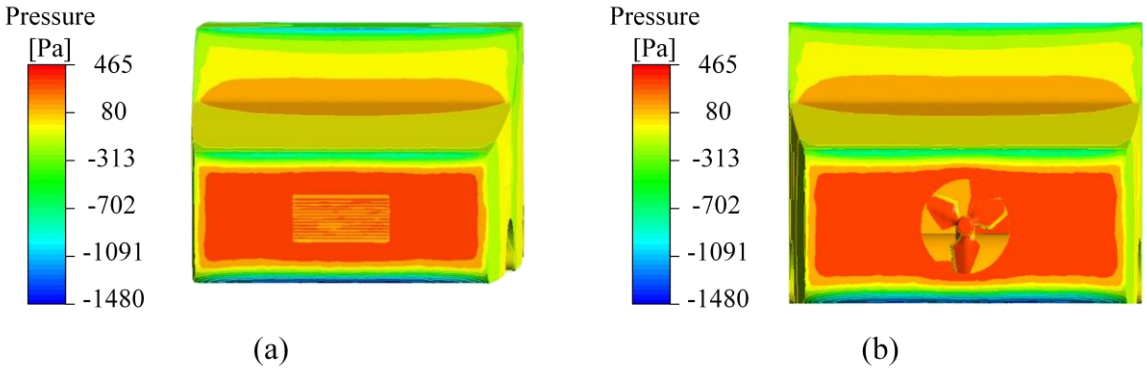

Figure 11. View of velocity vectors of MMV (a) isometric view, (b) front view.

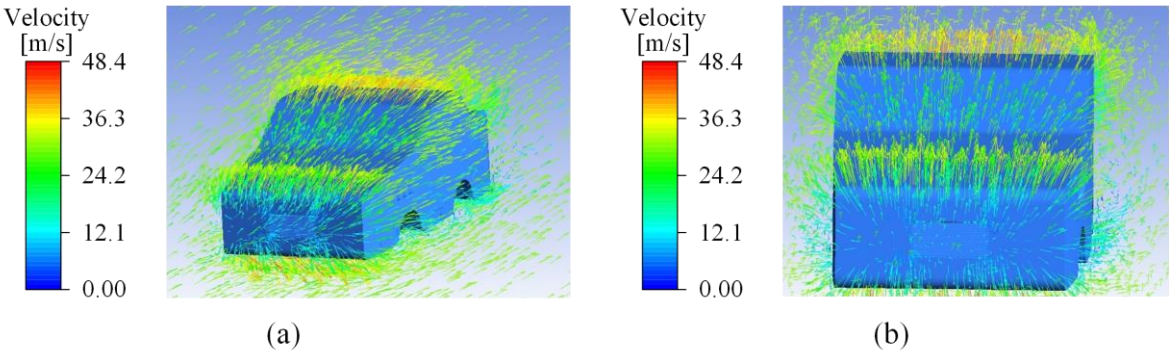

Figure 12. View of velocity vectors of VMWT (a) isometric view, (b) front view, (c) velocity vectors around the turbine.

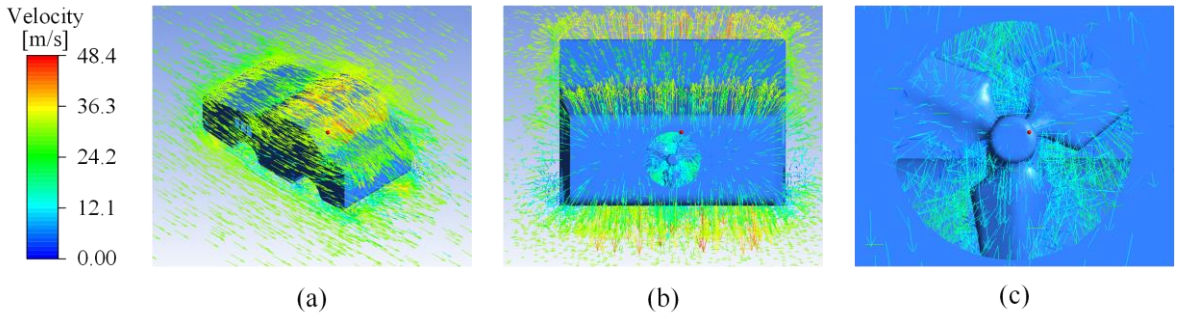

Figure 13. View of velocity streamlines of MMV (a) isometric view, (b) side view.

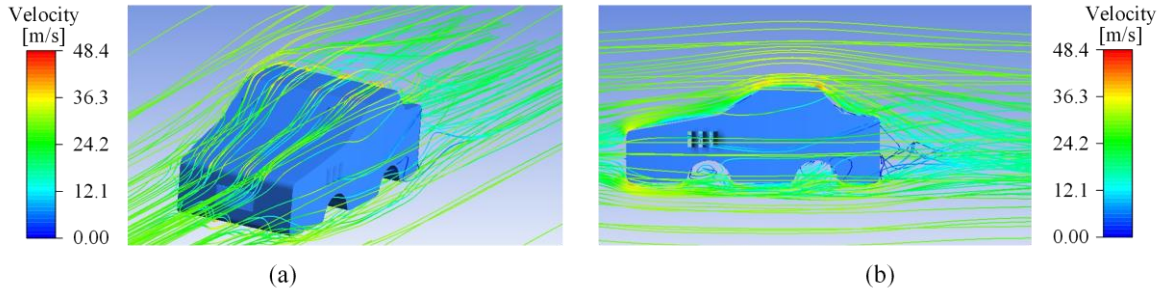

Figure 14. View of velocity streamlines of VMWT (a) side view, (b) front view, (c) velocity streamlines around the turbine.

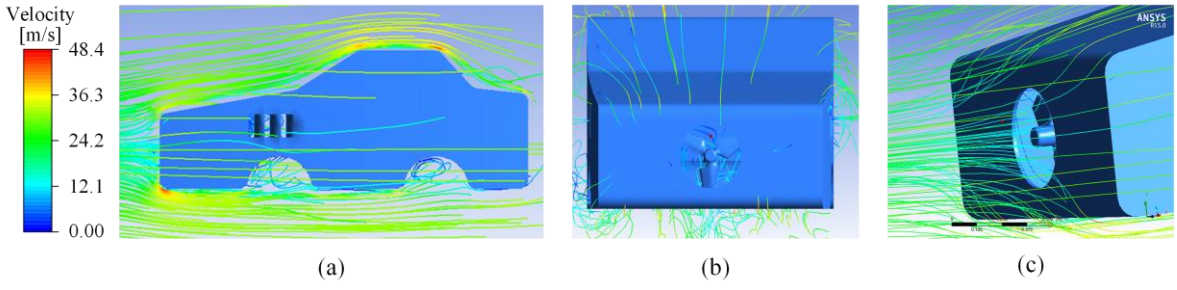

Figure 15. Pressure contour for (a) MMV, (b) VMWT.

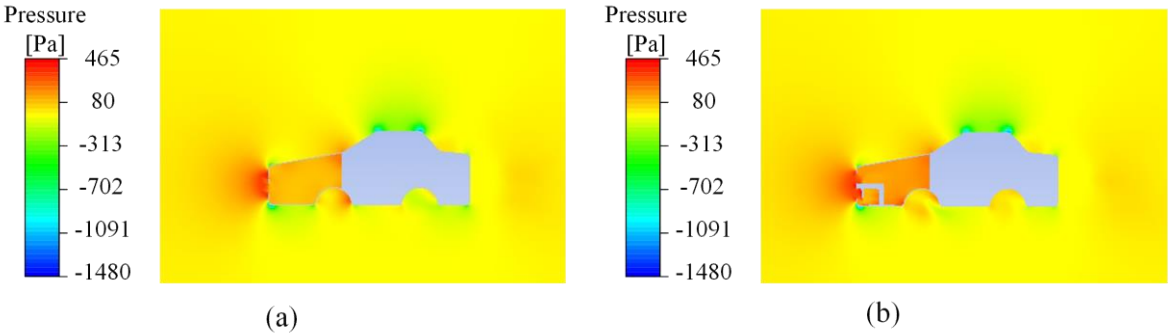

Figure 16. Velocity contour for (a) MMV, (b) VMWT.

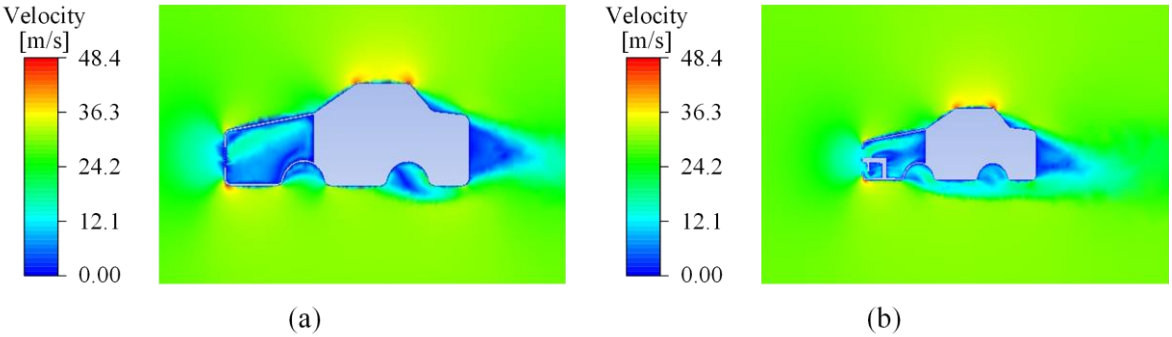

Figure 17. Aerodynamic energy loss of vehicle models.

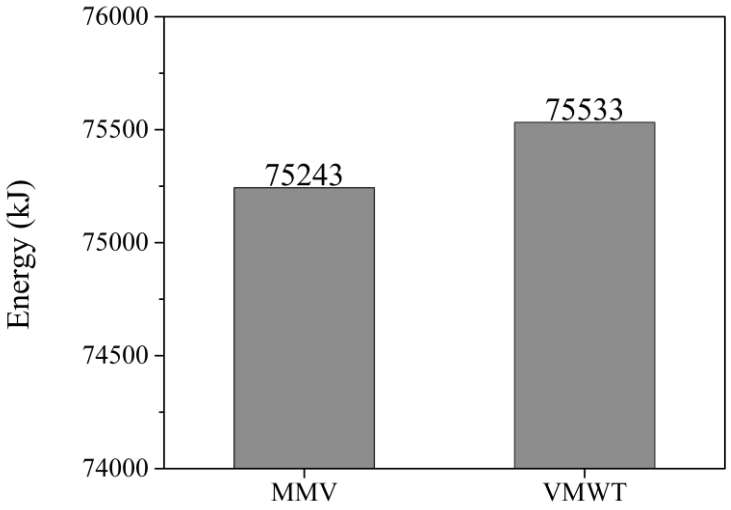

Figure 18. The amounts of energy.

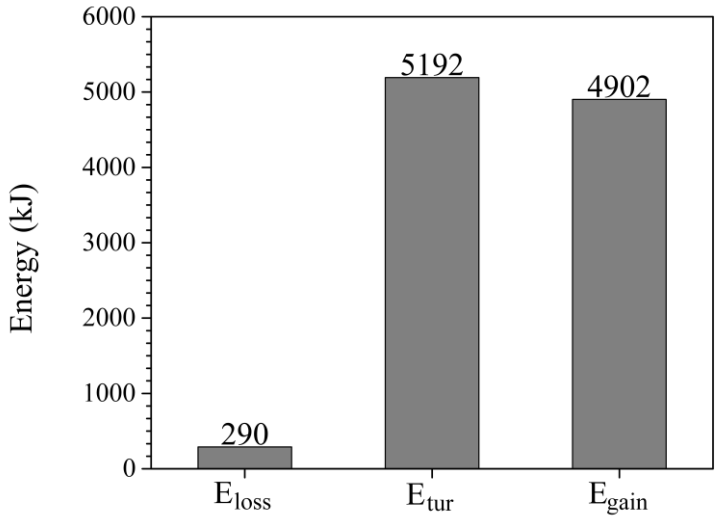

Figure 19. Aerodynamic energy loss and energy gain of VMWT compared to MMV.

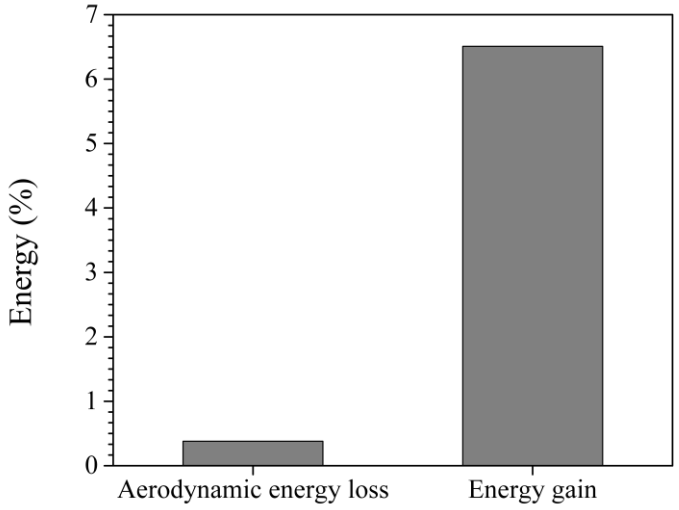

Table 1. Solution properties.

Parameter	Value
Dimension	3D
Solver Type	Pressure-Based
Velocity Formulation	Absolute
Time	Steady
Models	Viscous-Standard *k-ε*, Standard Wall Function
Density (kg/m^3)	1.225
Viscosity (kg/m.s)	1.789*10^{-5}

Table 2. Aerodynamic drag coefficient and aerodynamic drag force for vehicle models.

Vehicle Models	Drag Coefficient	Drag Force (N)
MMV	0.5693	752.43
VMWT	0.5715	755.33

Table 3. Technical specifications of the vehicle model.

Parameter	Value	Parameter	Value
Vehicle type	Basic passenger car	Projected surface area (m^2)	2.96
Length (mm)	4000	C_d	0.5693
Width (mm)	1810	C_l	0.2987
Height (mm)	1480	Vehicle speed (m/s)	27
Weight (kg)	1200	Distance traveled (km)	100